Journal of Tropical Resources and Sustainable Science
Website : http://journal.umk.edu.my/index.php/jtrss/
eISSN : 2462-2389
Vol: 14, Issue 2, 2026, 352-366
DOI: https://doi.org/10.47253/jtrss.v14i2.1737

RESEARCH ARTICLE

ADM1-based simulation of thermophilic biohydrogen production from enzymatically pretreated palm oil mill effluent

Ahmad Zul Izzi Fauzi [1,2,*], Muhammad Iqbal Ahmad [1,2], Azlina Mohammad Jais [3], Nik Nurul Anis Nik Yusuf [1,2], Sarizam Mamat [1,2] and Wan Mohd Faizal Wan Ishak [1,2]

[1] Faculty of Bioengineering and Technology, Universiti Malaysia Kelantan, Jeli Campus 17600 Jeli, Kelantan, Malaysia
[2] New Energy and Sustainable Research Group, Faculty of Bioengineering and Technology, Universiti Malaysia Kelantan, 17600 Jeli, Kelantan, Malaysia
[3] Energy Commission, No. 12, Jalan Tun Hussein Precinct 2, 62100, Putrajaya, Malaysia

ARTICLE HISTORY
Received : 23 September 2025
Accepted : 23 January 2026
Online : 30June 2026

KEYWORDS
dark fermentation;
enzymatic pretreatment;
volatile fatty acids (VFAs);
model calibration and validation;
sensitivity analysis;
Thermoanaerobacterium

☒ * **CORRESPONDING AUTHOR**
Dr. Ahmad Zul Izzi Fauzi
New Energy and Sustainable Research Group, Faculty of Bioengineering and Technology, Universiti Malaysia Kelantan, 17600 Jeli, Kelantan, Malaysia
Email: zulizzi.f@umk.edu.my

ABSTRACT

Palm oil mill effluent (POME) is an abundant agro-industrial wastewater with chemical oxygen demand (COD) exceeding 30,000 mg/L. While it holds promise as a substrate for sustainable biohydrogen production, its complex composition restricts microbial accessibility, resulting in low hydrogen yields. Moreover, empirical models such as the Gompertz equation provide good curve fitting but lack mechanistic depth, whereas default Anaerobic Digestion Model No. 1 (ADM1) formulations often underpredict volatile fatty acid (VFA) accumulation and hydrogen dynamics. This study aimed to calibrate and validate ADM1 for thermophilic biohydrogen production from enzymatically pretreated POME. Batch experiments were conducted under optimised conditions (pH 6.5, 4.3 % w/v enzyme loading, 55 °C), and the model was evaluated against experimental hydrogen evolution, reducing sugar release, and VFA profiles. Sensitivity analysis was performed to identify the key kinetic parameters that influence hydrogen production. Enzymatic pretreatment increased reducing sugar availability by approximately 182 %, resulting in a fivefold increase in cumulative hydrogen production (444 mL) compared with untreated POME. ADM1 simulations achieved high predictive accuracy ($R^2 > 0.90$; RMSE ≤ 0.2), successfully reproducing the trends in hydrogen evolution and VFA accumulation. The substrate uptake rate (2.47 kg COD kg^{-1} COD d^{-1}) and biomass decay constant (0.62 d^{-1}) emerged as critical drivers of hydrogen flux and microbial stability. This study demonstrates a validated application of ADM1 to thermophilic fermentation of enzymatically pretreated POME, establishing a robust mechanistic framework for process optimisation. Future work should extend this approach to continuous systems and hybrid ADM1–data-driven integration for scale-up and real-time monitoring.

1. INTRODUCTION

The increasing global demand for renewable energy has accelerated research into sustainable biohydrogen production as a clean alternative to fossil fuels. Biohydrogen generated through dark fermentation offers significant potential owing to its low energy requirement, rapid production rate, and ability to valorise organic waste streams. In tropical countries such as Malaysia, this approach aligns closely with national renewable energy and waste-to-energy strategies, as well as international sustainability commitments, including Sustainable Development Goal (SDG) 7 (Affordable and Clean Energy) and SDG 12 (Responsible Consumption and Production).

Palm oil mill effluent (POME), produced in large volumes during palm oil processing, is a high-strength wastewater with COD levels reaching up to 88,000 mg L^{-1} and poses severe risks of water pollution and greenhouse gas emissions if discharged untreated (Abdurahman et al., 2023). Malaysia alone generates tens of millions of tonnes of POME annually, making its effective treatment and valorisation a national environmental priority. Owing to its high carbohydrate and lipid content, POME represents a promising feedstock for hydrogenogenic fermentation, with reported yields of up to 2.3 mol H_2 mol^{-1} hexose equivalent under optimised conditions (Zainal et al., 2023). However, the complex composition of POME, dominated by lignocellulosic residues and recalcitrant organic compounds, limits direct microbial access to fermentable sugars, thereby constraining hydrogen production efficiency.

Enzymatic pretreatment has been shown to significantly enhance POME solubilisation, achieving more than 50 % higher reducing sugar release compared with

untreated samples (Deb et al., 2023). This pretreatment strategy is considered environmentally benign, as it operates under mild conditions and avoids the formation of inhibitory by-products typically associated with harsh chemical or thermal methods. Despite these advances, process optimisation remains challenging due to the complex and dynamic interactions between microbial consortia, substrate conversion pathways, and metabolite accumulation, necessitating the application of predictive modelling frameworks.

Previous studies on POME fermentation report substantial variation in hydrogen yields depending on pretreatment methods and operating conditions. Empirical models, such as the modified Gompertz equation, provide excellent statistical fits ($R^2 > 0.98$) but are limited in their ability to describe intermediate metabolites and mechanistic pathways (Wang & Guo, 2024). In contrast, ADM1 incorporates hydrolysis, acidogenesis, and VFA pathways, enabling mechanistic interpretation of anaerobic processes (Couto et al., 2022; Economou et al., 2024). However, simplified decay and inhibition terms in the default ADM1 formulation often led to discrepancies in predicting VFA accumulation, particularly acetate and propionate, under inhibitory or thermophilic conditions. (Segura et al., 2025).

Thermophilic systems generally outperform mesophilic digestion, achieving hydrogen yields of 1.8–2.3 mol H_2 mol^{-1} hexose compared with less than 1.2 mol H_2 mol^{-1} hexose under mesophilic operation. Nevertheless, thermophilic fermentation is often constrained by operational instability arising from pH fluctuations and excessive VFA accumulation (Singh et al., 2023). Comparative pretreatment studies indicate that dilute acid and heat/thermal methods substantially boost initial hydrogen yields (e.g., 1.24 mol H_2/mol glucose with acid pretreatment vs much lower in raw POME) (Mahmod et al., 2017), whereas enzymatic pretreatment typically provides more sustained hydrogen production under milder conditions, resulting in fewer inhibitory compounds (Izzi et al., 2023). These contrasting outcomes highlight the unresolved trade-off between maximising hydrogen yield and maintaining process stability, reinforcing the need for improved mechanistic modelling approaches.

Despite notable progress in POME valorisation, significant challenges remain in accurately predicting hydrogen yields under thermophilic conditions. Many studies continue to rely on empirical models that fail to capture microbial decay, inhibition, and intermediate metabolite dynamics, limiting their reliability during scale-up. Although ADM1 offers a mechanistic framework capable of simulating substrate hydrolysis, VFA fluxes, and hydrogen evolution, its default formulation underrepresents inhibition effects and decay kinetics, resulting in deviations exceeding 20 % in VFA prediction. Furthermore, most ADM1 calibration efforts have focused on mesophilic or mixed-substrate systems (Couto et al., 2020; Economou et al., 2024; Lee et al., 2022; Martínez-Mendoza et al., 2022), leaving a clear research gap in its application to thermophilic fermentation of enzymatically pretreated POME.

Therefore, this study aims to calibrate and validate the Anaerobic Digestion Model No. 1 (ADM1) for simulating thermophilic biohydrogen production from enzymatically pretreated palm oil mill effluent. The model is refined to capture substrate hydrolysis, reducing sugar dynamics, VFA accumulation, and hydrogen evolution under optimised batch fermentation conditions. Simulation outputs are validated against experimental data to assess predictive accuracy, identify parameter sensitivities, and elucidate inhibition and decay effects. The scope of this work includes (i) evaluation of enzymatic pretreatment effects on reducing sugar release, (ii) ADM1 calibration for thermophilic batch hydrogen production, and (iii) sensitivity analysis to identify critical kinetic parameters governing hydrogen yield. This mechanistic framework supports sustainable waste-to-energy development and strengthens biohydrogen process design for tropical agro-industrial wastewater.

2. MATERIALS AND METHODS

2.1. Substrate and Pretreatment

Palm oil mill effluent (POME) was collected from the discharge channel prior to the cooling pond at the Felda Global Ventures (FGV) palm oil mill, Malaysia. The raw POME was sieved through a 1 mm mesh to remove large particulates and stored at 4 °C prior to use. Initial characterisation indicated a total chemical oxygen demand (COD) of 42,580 mg L^{-1}, total solids (TS) of 24.6 g L^{-1}, and an initial pH of 4.3.

Enzymatic pretreatment was conducted using a cocktail of cellulase (120 FPU g^{-1}) following established enzymatic hydrolysis protocols for improving the biodegradability of complex agro-industrial wastewater (Deb et al., 2023; Izzi et al., 2023). The Box–Behnken Design (BBD) was employed to optimise three key parameters: enzyme concentration (1–5 % w/v), pH (5.0–7.5), and reaction time (6–24 h), in accordance with response surface methodology principles (Montgomery, 2017). Pretreatment experiments were performed in 250 mL Erlenmeyer flasks incubated in a shaking water bath (Julabo SW23, Germany) at 55 °C and 150 rpm. The optimised pretreatment condition was identified as 4.3 % (w/v) enzyme loading, pH 6.5, and a reaction time of 18 h.

2.2. Experimental Setup

Batch dark fermentation experiments were conducted in 500 mL serum bottles with a working volume of 400 mL, following standard protocols for batch hydrogen fermentation (Singh et al., 2023). Each reactor was sealed with butyl rubber stoppers and crimped aluminium caps, then flushed with high-purity nitrogen gas (99.99 %) for 5 min to establish anaerobic conditions. The fermentation substrate consisted of enzymatically pretreated POME, while the inoculum (15 % v/v) comprised thermophilic anaerobic sludge collected from a food waste digester located in Jungnam, Republic of Korea. A schematic overview of the experimental workflow is presented in Figure 1. All experiments were conducted under thermophilic conditions at 55 °C using a temperature-controlled incubator shaker (Thermo Scientific MaxQ™ 8000). The initial pH was adjusted using 1 M HCl or NaOH, and continuous mixing was maintained at 150 rpm. Operational variables, including initial COD concentration (30,000-45,000 mg L^{-1}), inoculum loading (10-15 % v/v), and initial pH (5.5-7.0), were optimised using Design-Expert® software (version 12, Stat-Ease Inc., USA).

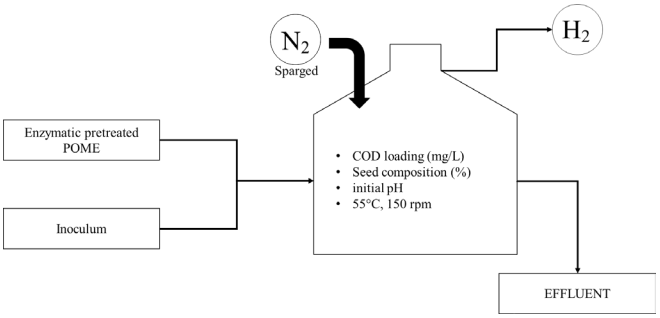

Figure 1: The diagram of thermophilic biohydrogen production process from pretreated palm oil mill effluent (POME).

2.3. Analytical Methods

Hydrogen gas production was quantified using gas chromatography (GC-TCD, Shimadzu GC-2014, Japan) equipped with a thermal conductivity detector and a stainless-steel column (2 m × 3 mm) packed with Porapak Q (Araujo et al., 2024). The injector and detector temperatures were maintained at 120 °C and 150 °C, respectively, with high-purity argon used as the carrier gas at a flow rate of 30 mL min^{-1}. Calibration was performed using certified hydrogen gas standards (99.999 %, Linde Gas).

Volatile fatty acids (VFAs), including acetate, butyrate, propionate, and valerate, were analysed by high-performance liquid chromatography (HPLC, Agilent 1260 Infinity) using a Rezex ROA-Organic Acid H^+ column (300 mm × 7.8 mm). The mobile phase consisted of 0.005 M H_2SO_4 delivered at 0.6 mL min^{-1}, with the column temperature maintained at 65 °C.

Reducing sugar concentrations were determined using the 3,5-dinitrosalicylic acid (DNS) method, with absorbance measured at 540 nm using a UV–visible spectrophotometer (Shimadzu UV-1800). COD, TS, volatile solids (VS), and pH were measured in accordance with Standard Methods for the Examination of Water and Wastewater (Rice et al., 2012).

2.4. Kinetic Modelling Using the Modified Gompertz Equation

The modified Gompertz equation was employed to describe cumulative biohydrogen production kinetics, as expressed in Equation (1). This model is widely applied for characterising batch dark fermentation behaviour (Wang & Guo, 2024).

$$H(t) = H_{\max} \cdot \exp\left\{-\exp\left[\frac{R_{\max} \cdot e}{H_{\max}}(\lambda - t) + 1\right]\right\} \quad (1)$$

where $H(t)$ represents cumulative hydrogen production (mL), H_{max} is the maximum hydrogen production potential (mL), R_{max} is the maximum hydrogen production rate (mL h^{-1}), λ denotes the lag phase duration (h), and t is the fermentation time (h). Gompertz parameters were estimated via nonlinear regression using Microsoft Excel® (Microsoft Corp., Seattle, WA, USA) and were employed to complement the mechanistic ADM1 analysis.

2.5. ADM1 Model Description and Modification

A modified version of the Anaerobic Digestion Model No. 1 (ADM1) was developed to simulate thermophilic dark fermentation (Keller et al., 2002). Methanogenesis pathways were excluded, and acidogenesis reactions were refined to prioritise hydrogenogenic pathways via monosaccharide and amino acid uptake (Couto et al., 2022).

The model was implemented in AQUASIM 2.1 (ETH Zurich, Switzerland) using a batch reactor configuration. Biochemical conversion pathways were represented by a system of ordinary differential equations incorporating stoichiometric matrices for soluble and particulate components. The model comprised 19 state variables and 12 kinetic rate equations governing reducing sugar degradation, VFA formation, and hydrogen evolution.

2.6. Parameter Estimation and Validation

Model calibration was performed using experimental data obtained under optimised batch fermentation conditions. Initial parameter values were adopted from the ADM1 framework (Batstone et al., 2002) and adjusted for thermophilic operation in accordance with reported literature (Lee et al., 2022). Sensitivity analysis identified the most influential kinetic parameters, including the maximum uptake rate for monosaccharides (km_{su}), half-saturation constant

(Ks_{su}), decay rate ($k_{dec,xsu}$), and hydrogen yield coefficient (Y_{h2_su}). Parameter estimation was conducted by minimising the sum of squared errors between simulated and experimental data using the Levenberg–Marquardt algorithm. Model performance was evaluated using the coefficient of determination (R^2), root mean square error (RMSE), mean bias error (MBE), and index of agreement (IOA). Validation confirmed strong predictive performance, with R^2 values exceeding 0.94 for reducing sugars, VFAs, and hydrogen evolution.

2.7. Microbial Community Analysis

Microbial community analysis was conducted to confirm the presence of hydrogen-producing microorganisms. Fermentation effluent corresponding to the highest hydrogen yield and butyrate-to-acetate ratio was collected and preserved at -20 °C prior to analysis. Total genomic DNA was extracted using the FastDNA™ SPIN Kit (MP Biomedicals, USA) following the manufacturer's protocol. PCR amplification was performed using universal bacterial primers 341F and 805R with Nextera adapters and Dr MAX DNA Polymerase (Doctor Protein, Korea). Sequencing was carried out using an Illumina MiSeq platform (Chunlab Inc., Seoul, Republic of Korea). Low-quality reads were removed prior to taxonomic classification using BLAST (NCBI). Sequences exhibiting >97 % similarity were aligned using MUSCLE in MEGA-X, and phylogenetic trees were constructed using the maximum likelihood method under the Jukes-Cantor model with 500 bootstrap replicates.

3. RESULT AND DISCUSSION

3.1 Reducing Sugar Recovery via Enzymatic Pretreatment

Enzymatic pretreatment plays a critical role in enhancing the hydrolysis of lignocellulosic residues in POME by converting complex polysaccharides into readily fermentable reducing sugars. Cellulase hydrolyses cellulose into glucose, amylase depolymerises residual starch into oligosaccharides, and protease releases soluble amino acids and peptides. Collectively, these actions increase the pool of fermentable substrates available for hydrogenogenic metabolism. Optimisation of key parameters, including enzyme dosage and pH, has been widely reported to significantly improve sugar recovery efficiency, thereby enhancing substrate availability for subsequent biohydrogen production.

As summarised in Table 1, optimisation at pH 6.5 resulted in a substantial enhancement of reducing sugar release, corresponding to an increase of approximately 182 % (mean ± SD) relative to the unoptimised baseline. All experimental values represent the mean of triplicate measurements, with standard deviations reported to reflect process variability. These findings are consistent with previous reports indicating that near-neutral pH conditions maximise biohydrogen production, where cumulative hydrogen yields increased markedly as pH was raised from acidic to near-neutral conditions due to improved microbial syntrophy and enhanced acetate–butyrate pathway activity (Martínez-Mendoza et al., 2022).

Table 1: Optimisation Conditions and Biohydrogen Yield from Pretreated POME

Variable	Unit	Range Tested	Optimised Value	Output (RS/H_2 Yield)
pH	–	5.0–7.5	6.5	RS: 182 ± 9 %[a]
Enzyme	% w/v	1–5	4.3	H_2: 444 ± 18 mL[b]
COD	mg/L	30k–45k	39,706	
Seed	%	10–15	13.64	

Values represent mean ± standard deviation (SD) of triplicate experiments (n = 3)
[a] RS: Reducing Sugar
[b] H_2: Hydrogen

Table 1 presents the optimal operating conditions and corresponding experimental outputs, while Figure 2 illustrates the response surface analysis depicting the interaction effects of enzyme concentration and pH on reducing sugar yield. The two representations are complementary rather than redundant, providing both numerical and visual insights into pretreatment optimisation.

An enzyme loading of 4.3 % (w/v) yielded the highest cumulative hydrogen production of 444 ± 18 mL, indicating an optimal balance between extensive polysaccharide hydrolysis and the avoidance of substrate inhibition. Similar trends have been reported for enzymatic pretreatment of carbohydrate-rich and lignocellulosic substrates, where increased fermentable sugar release directly translated into enhanced hydrogen yields during dark fermentation (Bouchareb et al., 2024). Notably, enzymatic pretreatment minimises the formation of inhibitory compounds compared with acid or thermal pretreatment, thereby sustaining microbial activity throughout fermentation (Sanghvi et al., 2024).

Optimisation of COD at 39,706 mg/L and seed inoculum at 13.64% ensured sufficient substrate availability and microbial activity without triggering substrate overload or acidification stress. This is consistent with evidence that a balanced substrate composition is critical for maintaining system stability, as unbalanced loading with excessive carbohydrates or fats can lead to rapid volatile fatty acid (VFA) and ammonium accumulation, impairing microbial performance and reducing gas yields. In contrast, balanced feedstocks supported stable microbial symbiosis, enabling 14–487% higher methane yields in solid-state anaerobic systems compared to unbalanced controls (Qi et al., 2023). Such results highlight that maintaining optimal substrate concentration and inoculum ratio prevents inhibitory

metabolite accumulation and secures favourable metabolic pathways for enhanced biohydrogen production.

As illustrated in Figure 2, reducing sugar yield was strongly influenced by both enzyme concentration and pH, with a maximum predicted value of approximately 8,500 mg L^{-1} achieved at higher enzyme loading (≈4.5 % w/v) and near-neutral pH. The response surface confirms that increased enzyme dosage is effective only within a narrow pH window, beyond which enzyme denaturation and reduced catalytic efficiency limit sugar release. At lower enzyme concentrations (<2.0 % w/v), reducing sugar yield declined sharply, indicating insufficient hydrolytic activity. Similarly, deviation from the optimal pH range led to lower reducing sugar release, highlighting the dual role of enzyme stability and microbial compatibility in optimising hydrolysis.

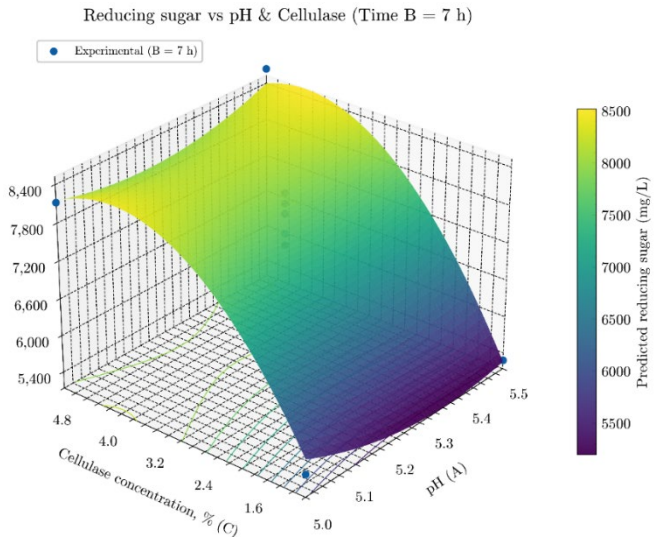

Figure 2: Response surface of reducing sugar yield as a function of enzyme concentration and pH.

The curved surface response confirms a significant interaction effect between pH and enzyme concentration. At optimized conditions, increasing enzyme dosage enhanced reducing sugar yield only when pH was controlled within the effective range. For example, Tween 80-assisted ethylene glycol pretreatment of sugarcane bagasse followed by enzymatic hydrolysis achieved a 25% increase in glucose yield (65.1% → 81.3%) at 5% surfactant loading and pH 5.0, whereas deviations from this pH resulted in lower hydrolysis efficiency despite higher enzyme concentrations (Song et al., 2024). Similarly, optimisation of alkali pretreatment for sweet sorghum residue demonstrated that a 2% NaOH pretreatment with 1 mm particle size improved cellulose digestibility to 62.7%, but sugar release declined under more severe or suboptimal conditions, underscoring the narrow operating window where enzyme loading is effective (Punia & Singh, 2024). Further optimization studies confirmed that enzyme efficiency is maximized within a narrow pH range, with cellulase performance significantly impaired under acidic or alkaline deviations (Porninta et al., 2024).

The increase in reducing sugars under optimized pretreatment conditions is directly linked to higher hydrogen recovery because sugar-rich hydrolysates preferentially drive metabolism toward the acetate–butyrate pathway. Acetate- and butyrate-dominant fermentations can yield up to 4 mol H_2/mol glucose and 2 mol H_2/mol glucose, respectively, compared to near-zero yields from propionate-dominated pathways (Yang et al., 2023). Sensitivity analyses further confirm that when acetate and butyrate account for most fermentation products, hydrogen yields increase by 7–35% compared to acetate–ethanol pathways (Singh et al., 2022). Experimental studies with mannitol-rich substrates also demonstrated that coupling acetate utilisation with butyrate formation enhances hydrogen selectivity and yield, achieving up to 91-100% butyrate selectivity with co-supplied acetate (Zhu et al., 2023).

3.2 Thermophilic Biohydrogen Production Performance

Under thermophilic conditions (55 °C), the batch dark fermentation of enzymatically pretreated POME yielded a cumulative hydrogen production of 444 ± 18 mL, representing a fivefold increase compared to untreated POME. The enhanced performance is attributed to increased reducing sugar availability and the activation of thermophilic hydrogen-producing consortia. The optimised process conditions of COD concentration of 39,706 mg/L, seed inoculum of 13.64%, and pH 6 were favoured the activation of hydrogen-producing thermophiles. As illustrated in Figure 3, pretreatment of POME markedly improves cumulative biohydrogen production relative to untreated POME.

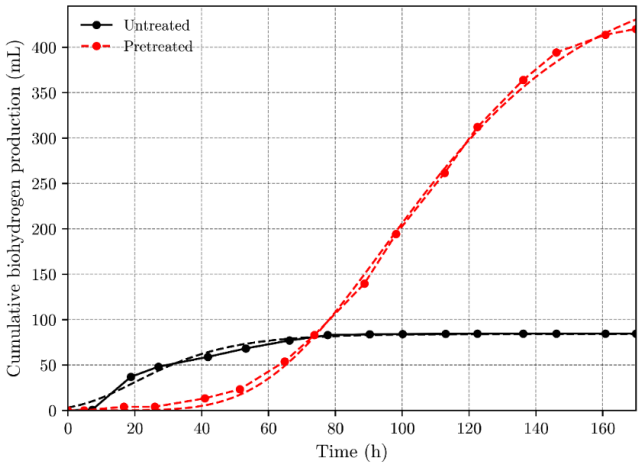

Figure 3: Cumulative biohydrogen production from untreated and pretreated POME over fermentation time. Pretreatment enhanced hydrogen yield, with a distinct exponential increase observed after 70 h, while the untreated substrate plateaued at 85 mL.

The untreated substrate yields 80-90 mL by 80 h and then levels off, suggesting substrate limitation or inhibition. In contrast, pretreated POME exhibits a lag phase (40–60 h), after which hydrogen production accelerates steeply, reaching over 400 mL by 160 h about 4-5× higher final yield than untreated. This behaviour is consistent with kinetic predictions from the modified Gompertz model, where pretreatment shortens the effective lag phase and increases the maximum hydrogen production rate (R_{max}).

Dilute acid pretreatment of POME has been shown to increase hydrogen yield by more than twofold, with cumulative volumes rising from 85 mL in untreated conditions to over 200 mL under optimised phosphoric acid pretreatment, owing to enhanced solubilisation and hydrolysis efficiency (S. Arisht et al., 2022). Similarly, thermal pretreatment has been reported to boost hydrogen production from ~120 mL to above 300 mL, primarily by inactivating hydrogen-consuming methanogens and increasing soluble carbohydrate release (Priambodo et al., 2024).

The lag phase observed in pretreated POME likely reflects the time required for microbial acclimatisation and enzymatic breakdown of complex organics before rapid fermentation commences. For example, in a study on thermal pretreatment of POME, no measurable hydrogen was detected until 24 h of incubation, after which hydrogen production increased sharply under optimal pretreatment conditions (100 °C), achieving a yield of 0.264 L H_2 / L-POME at 48 h, with COD removal of 22.74 % (Priambodo et al., 2024). In untreated POME, hydrogen production remained essentially undetectable over the same first 24 h (Priambodo et al., 2024). Additionally, a combined ultrasonication–microwave pretreatment of POME yielded 4,080 mL H_2 per L-POME, compared to 3,360 mL H_2 per L-POME for untreated raw POME (i.e. ~21 % higher cumulative yield), demonstrating that pretreatment shortens the adaptive phase and promotes faster hydrogen generation (Albuquerque et al., 2024).

Pretreatment of POME has been shown to increase cumulative biohydrogen yields by 1.5-fold to 2.35-fold over raw POME, depending on method and conditions; for example, 2.5 % (w/v) H_3PO_4 pretreatment produced 2.35× higher yield than untreated POME in batch fermentation (S. N. Arisht et al., 2022). Combining ultrasonication with microwave pretreatment reached 4080 mL H_2/L-POME vs ~3360 mL H_2/L-POME for raw substrate (≈1.21× increase), with COD removal efficiency ~75.6 % (Albuquerque et al., 2024). A hydrothermal pretreatment study reported 1.68-fold higher hydrogen production compared to untreated POME, along with reduced pollutant loads (Zainal et al., 2024).

3.3 Volatile Fatty Acid Profile and Metabolic Pathways

Analysis of the fermentation broth revealed a volatile fatty acid (VFA) profile dominated by butyric and acetic acids, indicating a favourable butyrate-type fermentation pathway. Acetate and butyrate together accounted for more than 80 % of total VFAs (mean ± SD), while propionate and valerate were present in relatively minor proportions. As illustrated in Figure 4A, acetate reached a concentration of approximately 45 mM (45 %), followed by butyrate at 35 mM (35 %). Propionate and valerate accounted for approximately 12 % and 8 % of the total VFA pool, respectively (Figure 4B). The low propionate concentration is particularly significant, as propionate formation consumes reducing equivalents and is known to suppress hydrogen generation. This acetate–butyrate dominance (80% of total VFAs) is consistent with the cumulative biohydrogen production trends observed in Figure 3, where pretreatment of POME led to a nearly fivefold increase in hydrogen yield (420 mL vs 85 mL for untreated).

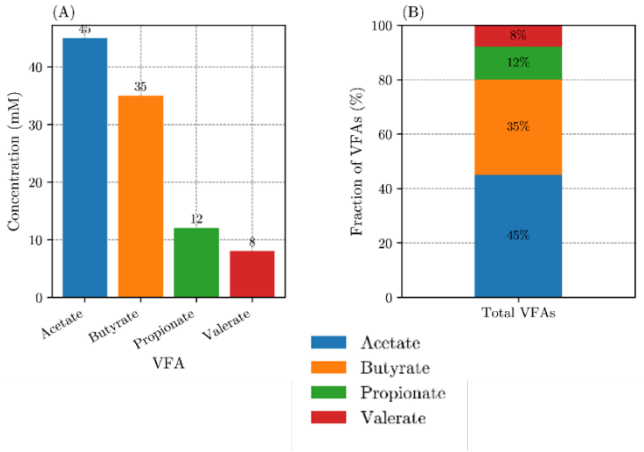

Figure 4: Distribution of volatile fatty acids (VFAs) during fermentation: (A) concentration of individual VFAs (mM); (B) fractional composition of VFAs (%). Acetate and butyrate dominate the VFA spectrum, followed by propionate and valerate.

The high acetate and butyrate fractions reflect a metabolic shift towards the acetate–butyrate fermentation pathway, which is strongly associated with higher hydrogen recovery. Recent studies confirm that mannitol fermentation (with acetate co-utilization) achieved 100% butyrate selectivity in the effluent and a hydrogen yield of 2.12 mol H_2 per mol mannitol, which increased further to 2.33 mol H_2 per mol mannitol when brown-algae hydrolysate was used (Li et al., 2022). Moreover, in-situ extraction of carboxylates increased the accumulated H_2 by 15% and butyrate molar yield by 71% relative to the control, indicating that relieving product inhibition and enriching butyrate pathways enhances H_2 recovery (Núñez-Valenzuela et al., 2024). Recent evidence shows that operating conditions that drive carbon flux into the propionate pathway (notably ORP ≈ −280 mV) suppress H_2

formation; conversely, avoiding propionate/lactate routes increases the likelihood of H_2 production via pyruvate-decarboxylation pathways (Sim et al., 2023). Mitigating product (carboxylate) build-up further raises accumulated H_2 by 15.2% and markedly increases butyrate yield (+71%), consistent with steering metabolism away from inhibitory/propionate routes and toward acetate–butyrate–H_2 pathways (Engliman et al., 2022). In the present case, propionate (12%) and valerate (8%) remained relatively low, indicating minimal hydrogen-consuming activity and supporting the enhanced yields shown in Figure 3.

The hydrogen yield improvement in Figure 3 and the acetate–butyrate enriched VFA profile in Figure 4 demonstrate that pretreatment not only increased substrate availability but also steered the metabolic balance toward pathways favourable for hydrogen generation. This provides mechanistic evidence that pretreatment strengthens both substrate solubilisation and metabolic efficiency, leading to higher cumulative hydrogen recovery.

As shown in Figure 5A, microbial community analysis revealed that *Thermoanaerobacterium* was the overwhelmingly dominant genus, accounting for 83% (29,455 reads) of the total population, followed by *Moorella* (9%), *Caldanaerobius* (3%), *Caloribacterium* (2%), and minor genera including *Ethanoligenens* and others (<2%). The dominance of *Thermoanaerobacterium* is consistent with its ability to thrive under thermophilic conditions and utilize diverse sugars for hydrogen production. Recent findings demonstrated that *T. thermosaccharolyticum* SP-H2 exhibited optimal growth at 55–60 °C and pH 7.5, producing hydrogen yields of up to 1.91 mol H_2/mol hexose (77.8 mmol H_2/L) from maltose, and comparable yields from galactose (201 ml H_2/g COD) and xylose (196 ml H_2/g COD) (Litti et al., 2022). Acetate and butyrate were identified as the main soluble metabolites, together constituting more than 60% of VFAs, and their accumulation showed a statistically significant positive correlation with hydrogen concentration and yield, confirming that the acetate–butyrate pathway is the most efficient metabolic route for biohydrogen generation in thermophilic systems (Litti et al., 2022). The relatively high abundance of *Moorella* suggests its contribution to acetate metabolism, as acetate was observed to be the dominant VFA during ammonia stress phases, with accumulation exceeding 600 mg/L when acetate metabolism was partially inhibited before recovery. Multi-omics analysis showed that acetate metabolism was initially suppressed due to downregulation of methyl-CoM reductase in Methanothrix, but the recovery of acetate turnover was facilitated by more tolerant taxa such as *Methanosarcina* and other acetate-utilizing bacteria (Zhang et al., 2022). In contrast, the low proportions of *Ethanoligenens* indicate that ethanol-type fermentation was not a significant route under these conditions, as ethanol accumulation was negligible compared to acetate and propionate fluxes, confirming the limited role of ethanol-type pathways in the tested system (Zhang et al., 2022).

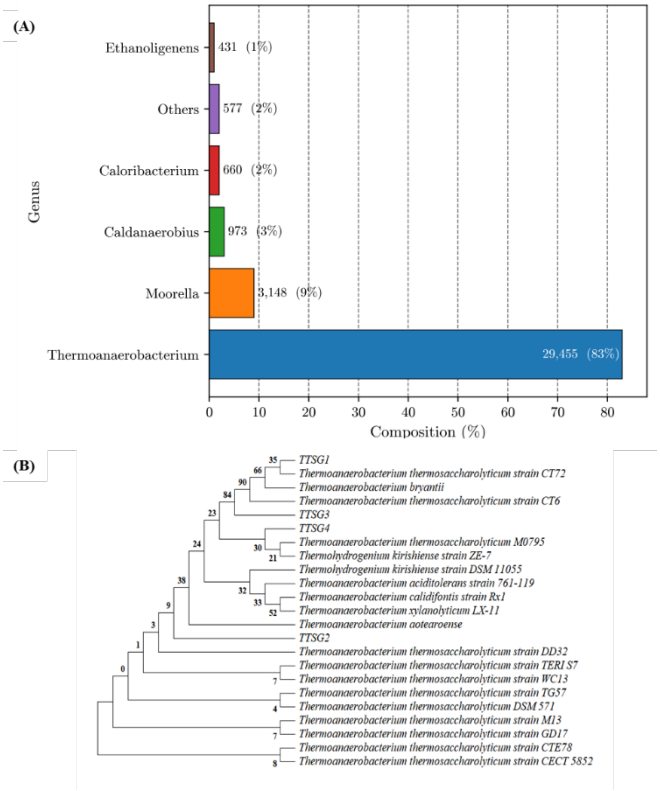

Figure 5: Microbial community structure and phylogenetic analysis of thermophilic biohydrogen-producing consortia: (A) relative abundance of dominant bacterial genera, and (B) phylogenetic tree showing the taxonomic relationship of *Thermoanaerobacterium* with other closely related strains.

The phylogenetic tree in Figure 5B confirmed that the enriched strains clustered closely with *Thermoanaerobacterium thermosaccharolyticum*, *Thermoanaerobacterium xylanolyticum*, and other well-characterized hydrogen producers. This microbial evidence reinforces the kinetic and VFA-based findings, establishing a coherent link between pretreatment, microbial selection, metabolic routing, and hydrogen production. In thermophilic enrichment studies, *Thermoanaerobacterium* lineages consistently dominated microbial consortia due to their ability to degrade complex polysaccharides and channel metabolism toward the acetate–butyrate pathway. For example, in Fe–Mn impregnated biochar systems, the combined relative abundance of *Thermoanaerobacterium*, *Anaerocolumna*, and *Thermosinus* reached 84.12 %, which was 25.63 % higher than the control group, supporting superior hydrogen yields of 1.71 mL H_2/mL-culture and 586.19 mL H_2/g-carbohydrate (Chen et al., 2023). Similarly, thermophilic operating environments enriched hydrogen-producing taxa such as

Thermoanaerobacterium and *T. thermosaccharolyticum*, which showed high tolerance to elevated temperatures and efficient carbohydrate utilization, resulting in hydrogen yields exceeding 2.0 mol H_2/mol hexose under optimized pretreatment conditions (Ndayisenga et al., 2022). These findings reinforce that phylogenetic clustering with *Thermoanaerobacterium* species reflects both taxonomic proximity and functional specialization in thermophilic biohydrogen production.

3.4 ADM1 Model Calibration and Validation

Accurate calibration and validation of the Anaerobic Digestion Model No. 1 (ADM1) are essential to ensure that kinetic parameters reliably represent substrate degradation, microbial dynamics, and metabolite fluxes in complex waste streams such as POME. As summarised in Table 2, the calibrated ADM1 model reproduced the experimental hydrogen evolution profiles with high accuracy, achieving an R^2 of 0.96 and a low RMSE ≤ 0.2. These results indicate excellent agreement between simulated and experimental data. The strong predictive capability indicates that the selected kinetic constants effectively captured substrate hydrolysis, acidogenesis, and hydrogenogenic conversion dynamics.

Table 2: Kinetic Parameters and Validation Indicators for ADM1-Based Model.

Parameter	Symbol	Value	Unit
Max uptake rate	km_{su}	2.47	kg COD/kg COD/day
Half-saturation constant	Ks_{su}	1.17	kg COD/m³
Decay rate	k_{dec_Xsu}	0.62	1/day
R^2 (H_2 evolution)	–	0.96	–
RMSE[a] (H_2 prediction)	–	≤ 0.2	–

[a] RMSE: Root mean square error

The calibrated maximum substrate uptake rate (km_{su} = 2.47 kg COD·kg^{-1} COD·day^{-1}) reflects the high metabolic activity of acidogenic consortia under optimised pretreatment and thermophilic conditions. This high uptake rate reflects the strong metabolic activity of acidogenic consortia under optimized pretreatment. Reported km_{su} values for carbohydrate-rich substrates typically range from 1.5 to 3.0 kg COD·kg^{-1} COD·day^{-1}, suggesting that the obtained value is consistent with efficient acidogenesis (Mo et al., 2023). Similar uptake constants (2.0–2.8) were also observed in ADM1-based calibrations for food waste digestion, confirming that the calibrated value of 2.47 is consistent with efficient acidogenesis under optimized conditions (Economou et al., 2024). The half-saturation constant describes microbial affinity for substrates. Values between 0.5–2.5 kg COD·m^{-3} have been reported for sugar and amino acid degraders, with lower values (<1.5) indicating strong substrate affinity (Mo et al., 2023). Model calibrations in wastewater and sludge digestion similarly reported Ks_{su} values around 1.0–1.3, confirming that the obtained 1.17 reflects robust substrate utilization at moderate COD levels (Emebu et al., 2022). Decay constants (k_{dec_Xsu}) for acidogenic biomass generally range 0.2–0.8 day^{-1}, influenced by stress factors such as VFA accumulation or low pH (Mo et al., 2023). The calibrated value of 0.62 day^{-1} lies within this reported range, reflecting moderate stress but stable microbial retention. Comparable decay rates (0.5–0.7 day^{-1}) have been observed in ADM1 calibrations under high organic loading (Economou et al., 2024) and in bioreactor studies where VFA buildup accelerated biomass turnover (Anjum et al., 2023).

As shown in Figure 6, the ADM1 simulation reproduced the experimental hydrogen evolution trend with a high coefficient of determination (R^2 = 0.903) and a very low prediction error (RMSE = 4.82 × 10^{-5}). The model accurately captured the rapid increase in hydrogen volume during the first 48 hours, followed by a slower rise approaching a plateau beyond day 3. This pattern reflects the typical fermentation dynamics in pretreated POME systems, where rapid hydrolysis and acidogenesis dominate early, while hydrogen yields stabilize once substrate availability declines.

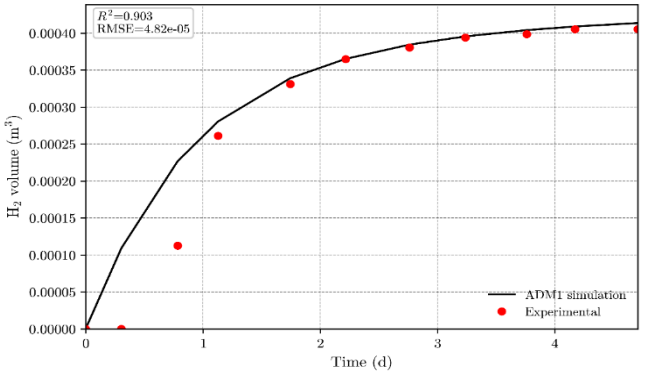

Figure 6: Comparison of ADM1-simulated hydrogen evolution with experimental data under optimized fermentation conditions. The close agreement between simulation (solid line) and experimental results (red points) demonstrates the predictive accuracy of the calibrated ADM1 model.

The simulated maximum hydrogen volume of 0.0004 m³ closely matched the experimental endpoint, demonstrating that the calibrated kinetic parameters effectively represented substrate uptake, microbial activity, and decay processes. Comparable studies have reported R^2 values above 0.90 for ADM1 calibrations of carbohydrate-rich feedstocks, highlighting the model's robustness when kinetic constants are tuned for system-specific conditions (Bayu et al., 2022; Bechara, 2022).

The predictive accuracy observed here is consistent with recent evidence that ADM1 modifications and careful parameter calibration can reliably capture not only hydrogen

yields but also VFA accumulation and microbial stress responses (Bechara, 2022; Emebu et al., 2022). Furthermore, the low RMSE suggests the model could serve as a reliable decision-support tool for scaling up pretreatment strategies and controlling fermentation stability in biohydrogen systems.

3.5 Comparative Analysis of ADM1 and Gompertz Models

ADM1 accurately reproduced hydrogen evolution (R^2 = 0.96), while the Gompertz model provided superior curve-fitting (R^2 = 0.993), confirming their complementary roles. While Gompertz-based kinetics provide excellent curve-fitting for cumulative hydrogen production, ADM1 captures the underlying biochemical and microbial mechanisms, making such side-by-side assessments valuable for both validation and process optimization.

As illustrated in Figure 7, the hydrogen production profile from cellulase-pretreated POME under thermophilic conditions was well described by both the Gompertz model and the ADM1 simulation, when compared against the experimental dataset. The Gompertz model achieved excellent predictive performance with R^2 = 0.993, RMSE = 1.28×10^{-5}, and MAE = 1.08×10^{-5}, outperforming the ADM1 simulation of R^2 = 0.903, RMSE = 4.82×10^{-5} and MAE = 2.49×10^{-5}. These results indicate that while ADM1 is effective for mechanistic representation of microbial and biochemical processes, empirical models such as Gompertz provide superior curve-fitting ability for cumulative hydrogen evolution.

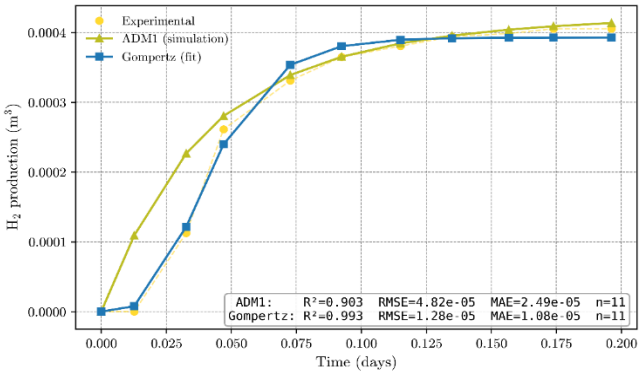

Figure 7: Comparison of ADM1-simulated hydrogen evolution with experimental data under optimized fermentation conditions. The close agreement between simulation (solid line) and experimental results (red points) demonstrates the predictive accuracy of the calibrated ADM1 model.

The hydrogen production profile exhibited three distinct phases: (i) a short lag phase (<0.03 d), (ii) a rapid exponential hydrogen evolution phase between 0.03-0.10 d, and (iii) a plateau phase beyond 0.15 d associated with substrate depletion and metabolic stabilisation. The higher accuracy of the Gompertz model in capturing the transition between exponential growth and plateau is supported by recent kinetic studies. Multiscale kinetic modelling applied to membrane bioreactors reported R^2 values exceeding 0.99 across 11 case studies, demonstrating superior curve-fitting performance compared to conventional Gompertz and logistic models (Asvad et al., 2023). Similarly, batch dark fermentation systems fitted with modified Gompertz models consistently achieved R^2 > 0.98 when predicting cumulative hydrogen evolution, confirming its robustness in describing dark fermentation kinetics (Martínez et al., 2022).

Despite its slightly lower statistical performance, ADM1 offers significant advantages by explicitly representing substrate uptake, microbial growth, and decay kinetics, making it more suitable for process optimization and scenario testing. Recent ADM1 improvements that incorporated inhibition dynamics and thermophilic kinetic adjustments have shown strong predictive performance, with model validation against experimental hydrogen evolution achieving R^2 values of 0.91–0.95 and low RMSE (<0.05), confirming the capability of calibrated ADM1 structures to reproduce cumulative H_2 production trends under thermophilic conditions (Bayu et al., 2022; Bechara, 2022). Thus, combining mechanistic and empirical modelling approaches enhances both predictive accuracy and interpretability.

3.6 Sensitivity Analysis and Parameter Estimation

Sensitivity analysis was performed to identify the kinetic and stoichiometric parameters exerting the greatest influence on hydrogen evolution and metabolite dynamics within the ADM1 framework. This analysis provides mechanistic insight into pathway dominance and ensures that calibration efforts focus on parameters most relevant to process optimisation.

As shown in Figure 8, hydrogen production and VFA profiles were most sensitive to the maximum substrate uptake rate (km_{su}) and the half-saturation constant (Ks_{su}). This finding mechanistically links enzymatic pretreatment (enhanced sugar release) to increased hydrogen evolution via accelerated acidogenesis. The strong positive sensitivity of acetate (Figure 8A) and butyrate (Figure 8C) to km_{su} indicates that accelerated substrate hydrolysis and fermentation promote pathways favourable for hydrogen production. In contrast, propionate (Figure 8B) and valerate (Figure 8D) exhibited weaker sensitivity, suggesting that these hydrogen-consuming pathways are less directly driven by substrate uptake kinetics.

The sensitivity of reducing sugar degradation (Figure 8E) further highlights the importance of Ks_{su} in regulating substrate affinity. A lower Ks_{su} value sustains higher substrate uptake at moderate COD levels, preventing sugar accumulation and ensuring continuous VFA and hydrogen generation.

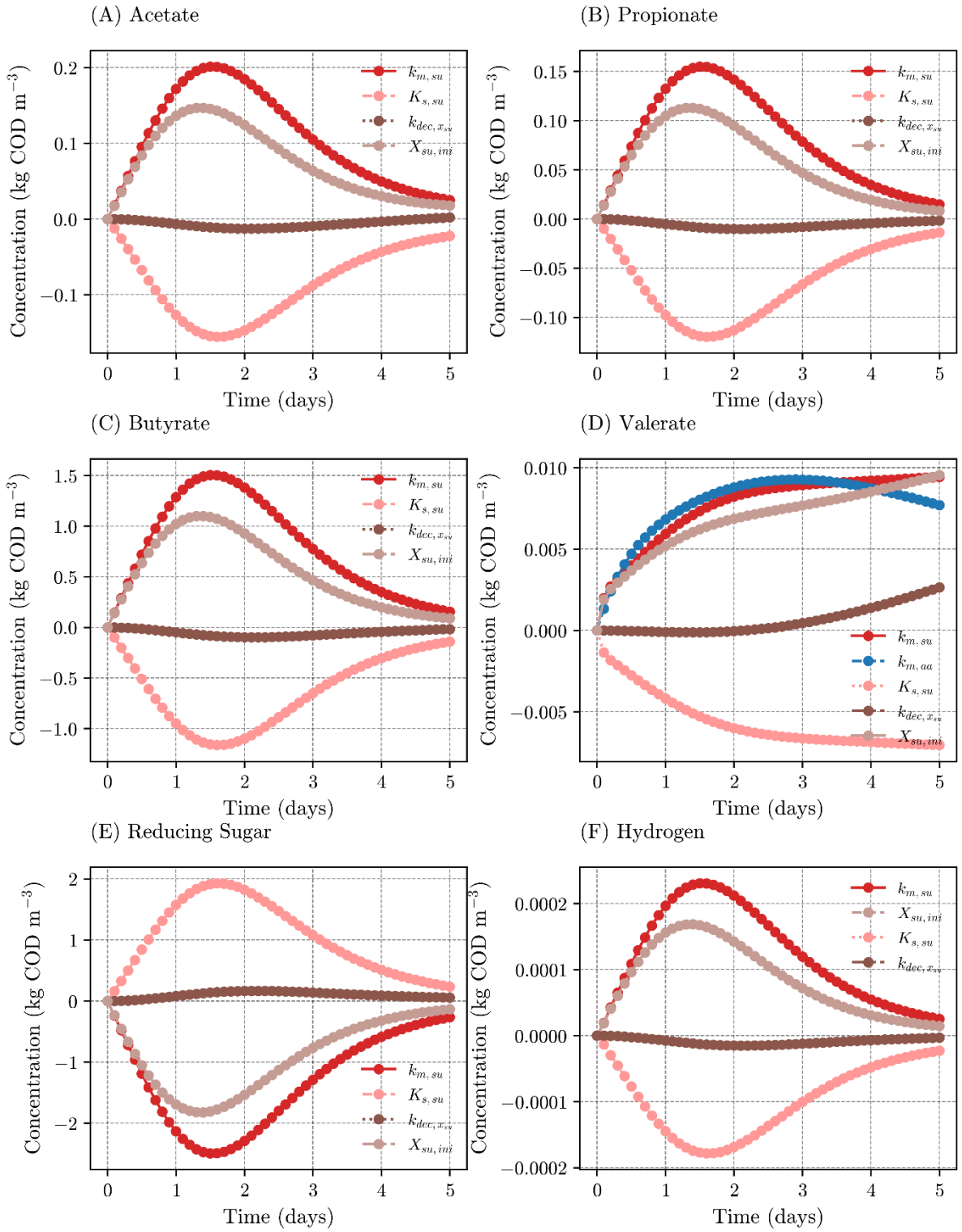

Figure 8: Sensitivity function of kinetic and stoichiometric parameters on metabolite dynamics: (A) acetate, (B) propionate, (C) butyrate, (D) valerate, (E) reducing sugar degradation in the reactor compartment, and (F) hydrogen evolution in the headspace.

This finding is consistent with mechanistic ADM1-based modelling of anaerobic membrane bioreactors treating high-strength wastewater, where sugar- and amino acid-rich influents generated the highest hydrogen production rates (5.9–6.1 L H_2 $L^{-1}{\cdot}d^{-1}$), confirming that reducing sugar availability is a critical driver for downstream VFA formation and hydrogen fluxes (Vera et al., 2023). In contrast, lipid-rich influents produced only 0.7 L H_2 $L^{-1}{\cdot}d^{-1}$, highlighting the comparatively limited hydrogenogenic potential of lipid pathways under similar conditions (Vera et al., 2023). Recent ADM1 improvements, incorporating additional metabolic pathways such as acrylate and homoacetogenesis, have demonstrated a strong predictive capability, with calibration against sugarcane vinasse acidogenesis showing R^2 values

above 0.95 for hydrogen, acetate, and propionate trends at 15–20 kg COD·m^{-3}. The inclusion of lactate-to-propionate conversion and hydrogen consumption via homoacetogenesis was critical for accurately capturing reducing sugar degradation and downstream VFA fluxes, confirming the central role of sugar and lactate pathways as system drivers (Couto et al., 2022).

Hydrogen sensitivity (Figure 8F) showed a pronounced dependence on km_{su}, confirming that microbial metabolic activity, rather than decay parameters alone, governs gas evolution. Global sensitivity analysis under mixed aleatory and epistemic uncertainties has demonstrated that perturbations in key kinetic and operating parameters can substantially impact system performance. In the hydrogenation of levulinic acid and butyl levulinate to γ-valerolactone, variations in initial temperature, Ru/C catalyst loading, and hydrogen pressure accounted for the largest share of variance in both thermal risk and production rate, with Sobol indices exceeding 0.25–0.35 for these parameters. This indicates that yield and risk metrics can shift by more than 20% under parameter uncertainty, underscoring the necessity of precise calibration of uptake-related constants and operating conditions (Shi et al., 2024). Meanwhile, the decay rate (k_{dec_Xsu}) exerted moderate influence on all metabolites, reflecting its role in biomass turnover and system stability. High decay rates accelerate biomass loss and reduce hydrogen generation, as confirmed by ADM1-based simulations of agro-industrial waste co-digestion. In continuous CSTR systems, model calibration showed that the first-order biomass decay rate ($k_{dec,all}$) of 0.02 d^{-1} significantly influenced microbial stability, with elevated decay leading to lower carbohydrate consumption and reduced hydrogen fluxes at short HRTs (0.75 d). The model further demonstrated that excessive decay promotes acetate and ethanol accumulation while suppressing stable hydrogenogenic activity, emphasizing the importance of balancing biomass growth and washout (Economou et al., 2024).

3.7 Implications and Limitations

Mechanistic validation with ADM1 clarifies which pathways govern hydrogen release and where operational bottlenecks arise for scale-up (e.g., short HRTs, pH/VFA inhibition). Recent work shows ADM1 can capture hydrolysis–acidogenesis dynamics for complex agro-industrial wastes yet fits to intermediates (VFAs) may degrade if inhibition terms and parameter estimation are not carefully treated, highlighting the need for targeted calibration and explicit inhibition functions.

As illustrated in Figure 9B–C, hydrogen and carbon dioxide were the dominant gases produced, with sharp increases during the first day followed by a gradual decline. The gas composition stabilized at approximately 40% H_2 and 60% CO_2, with negligible methane formation, indicating that the system was operating under acidogenic conditions. This trend is consistent with controlled dark fermentation studies where only H_2 and CO_2 were detected, and no methane was observed across all operational ranges, confirming the effective suppression of hydrogenotrophic methanogens. At pH 6.0 and a hydraulic retention time (HRT) of 3 h, the maximum hydrogen production rate reached 11.4 L H_2/L^{-d}, with hydrogen comprising 59–75% of the total biogas, demonstrating that thermophilic or controlled pH regimes can sustain hydrogen-dominant gas composition while excluding methanogenesis (Zagrodnik et al., 2022).

The COD profiles in Figure 9D demonstrate that while total COD decreased slightly from ~32 to ~31.5 kg COD·m^{-3}, soluble COD increased in the early stages due to substrate solubilization before levelling off as reducing sugars were consumed. This pattern is consistent with ADM1-based co-digestion simulations of sewage sludge, where influent COD was fractionated into ~40% inert particulate, 30% hydrolysis products, and 30% degradable particulates. During digestion, soluble COD values rose to 6,921 mg/L as complex particulates disintegrated, before stabilizing as VFAs and methane were produced (Mudzanani et al., 2023). The model validation confirmed that effluent COD trends closely tracked experimental observations, demonstrating that COD fractionation and solubilization are critical to predicting substrate availability and subsequent gas yields (Mudzanani et al., 2023).

Biomass dynamics presented in Figures 9A and 9E show that hydrolytic and acidogenic populations exhibited the fastest growth during the first 24 h, reaching peak concentrations of ~3.2 kg COD·m^{-3}, before stabilizing as substrate availability declined. In contrast, hydrogenotrophic and methanogenic groups remained below 0.2 kg COD·m^{-3} throughout the run, confirming suppression of hydrogen-consuming pathways under thermophilic conditions. These trends are consistent with ADM1-based co-digestion studies, where short HRTs (1–2 d) enriched acidogenic bacteria, while methanogens were inhibited, leading to gas compositions dominated by H_2 and CO_2 (Economou et al., 2024).

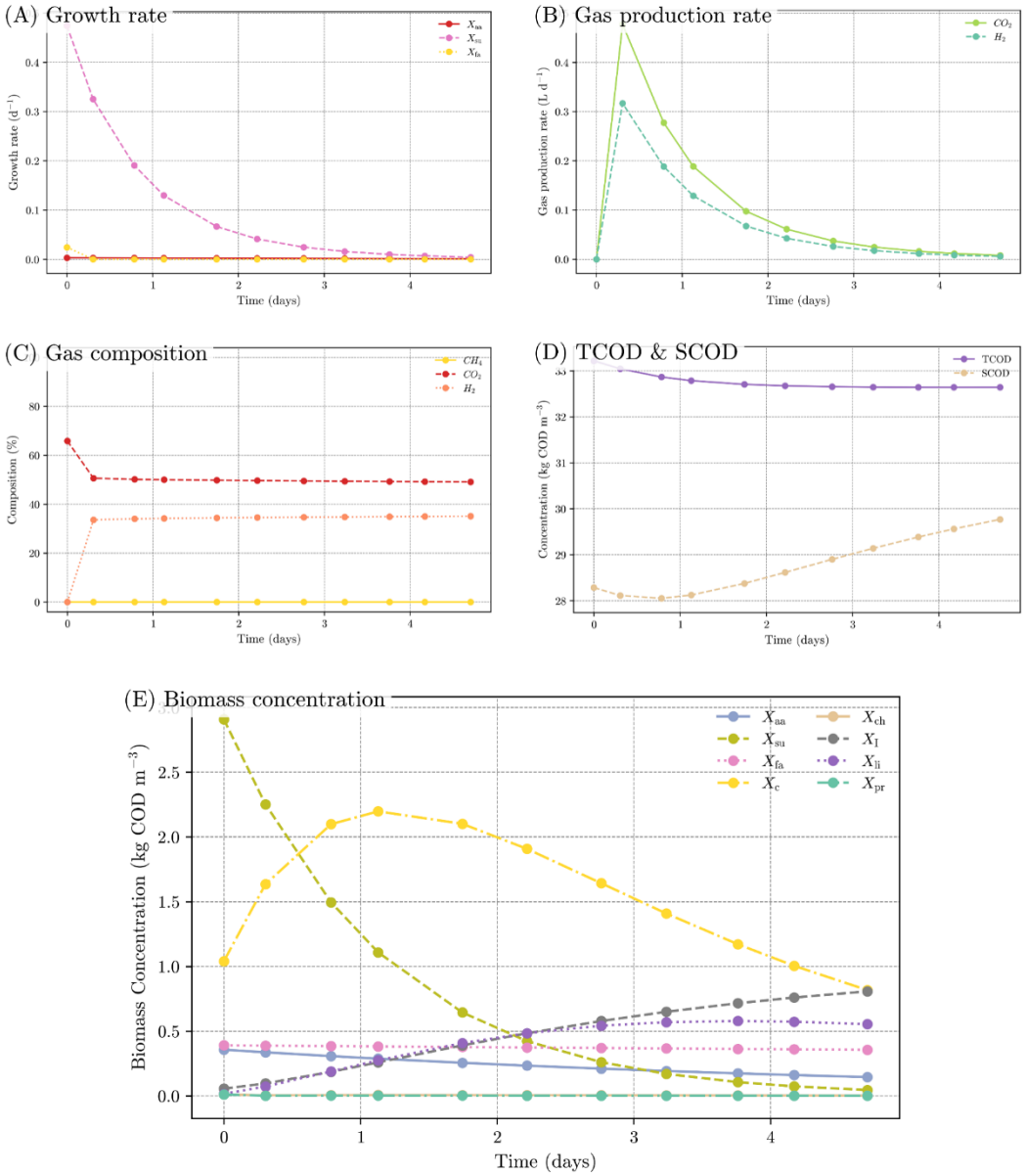

Figure 9: Integrated ADM1 outputs for thermophilic dark fermentation of pretreated POME: (A) Growth rates of key functional groups; (B) Gas production rates (H_2, CO_2); (C) Gas composition (vol%); (D) TCOD and SCOD profiles; (E) Biomass state variables (kg COD·m^{-3}).

Acidogenic biomass plateaued beyond 48 h, indicating a metabolic transition from exponential growth to maintenance. Meanwhile, inert and particulate fractions (XI, XPr, XCh) accumulated progressively, with inert biomass rising from ~1.5 to 2.3 kg COD·m^{-3}. This accumulation reflects endogenous decay, a phenomenon confirmed in ADM1 model calibrations where decay constants (k_{dec} ≈ 0.02–0.62 d^{-1}) significantly influenced long-term microbial stability (Mo et al., 2023). Failure to account for such decay pathways often results in overprediction of active biomass and hydrogen yield, highlighting the necessity of including accurate decay kinetics in ADM1 simulations (Dareioti et al., 2014).

The simulation results highlight that reducing sugar uptake primarily directed carbon flux toward the acetate–butyrate pathway, leading to efficient hydrogen release. This observation is consistent with thermophilic anaerobic fermentation of carbohydrate-rich food waste, where butyrate (65.4%) and acetate (24.2%) dominated the short-chain fatty acid spectrum, while hydrogen yields reached 98.8 mL H_2 g CODfed^{-1} (157 L H_2 kg VSfed^{-1}) (Greses et al., 2022). The early surge in hydrogen production followed by a decline corresponds to substrate depletion and accumulation of VFAs, particularly butyrate, which has been reported as the major metabolic endpoint under slightly acidic thermophilic conditions (pH 5.8). This metabolic pattern reflects the shift toward the acetate–butyrate pathway as the primary hydrogenogenic route, a well-recognized feature of dark fermentation systems processing carbohydrate-rich substrates (Greses et al., 2022).

Finally, the combined reproduction of growth rates,

gas composition, COD fractions, and biomass dynamics confirms the robustness of the calibrated ADM1 framework for pretreated POME. This finding aligns with broader process simulation studies, where scaled-up biocatalytic systems demonstrated that well-parameterized models can capture macroscopic performance trends and provide valuable insights for industrial translation (Chen & Wang, 2024). However, the results also emphasize the limitations of simplified decay and inhibition terms. Reviews on hybrid modelling approaches highlight that conventional mechanistic models often misrepresent intermediate metabolites and microbial dynamics when inhibition kinetics are oversimplified, whereas hybrid frameworks combining mechanistic cores (such as ADM1) with data-driven layers improved prediction accuracy and robustness during scale-up (Albino et al., 2024).

4. CONCLUSION

This study successfully calibrated and validated the Anaerobic Digestion Model No. 1 (ADM1) for simulating thermophilic biohydrogen production from enzymatically pretreated palm oil mill effluent. The model was applied under batch conditions, integrating pretreatment-enhanced reducing sugar availability, substrate hydrolysis, volatile fatty acid (VFA) accumulation, and hydrogen evolution. The findings confirm that Enzymatic pretreatment of POME enhanced reducing sugar release by ~182%, enabling cumulative hydrogen yields of 444 mL, nearly fivefold higher than untreated POME. The calibrated ADM1 reproduced experimental hydrogen dynamics with strong accuracy (R^2 > 0.90; RMSE ≤ 0.2), validating key kinetic parameters such as substrate uptake rate (2.47 kg COD·kg^{-1} COD·d^{-1}) and decay constant (0.62 d^{-1}). Sensitivity analysis further revealed that reducing sugar availability and uptake kinetics were the primary drivers of acetate–butyrate pathway dominance and hydrogen release, while elevated decay rates accelerated inert biomass accumulation and curtailed yields. Overall, the study demonstrates the novelty of applying ADM1 to thermophilic, enzymatically pretreated POME, providing a mechanistic tool for optimizing biohydrogen systems and informing scale-up strategies, with future work directed toward continuous validation and hybrid mechanistic–data-driven integration.

ACKNOWLEDGEMENT

The authors gratefully acknowledge the Water-Energy Nexus Laboratory, University of Seoul, for providing the research facilities necessary for data acquisition. Financial support from the Korea Institute of Energy Technology Evaluation and Planning (KETEP) and the Ministry of Trade, Industry and Energy (MOTIE), Republic of Korea, under Grant No. 20173010092510, is sincerely appreciated. This study was also supported by the Ministry of Higher Education, Malaysia, through the Fundamental Research Grant Scheme (FRGS-EC/1/2024/TK08/UMK/02/4).

REFERENCES

Abdurahman, N. H., Rosli, Y. M., Azhari, N. H., Hayder, G., & Norasyikin, I. (2023). A Hybrid Ultrasonic Membrane Anaerobic System (UMAS) Development for Palm Oil Mill Effluent (POME) *Treatment. Processes, 11*(8), 2477. https://www.mdpi.com/2227-9717/11/8/2477

Albino, M., Gargalo, C. L., Nadal-Rey, G., Albæk, M. O., Krühne, U., & Gernaey, K. V. (2024). Hybrid Modeling for On-Line Fermentation Optimization and Scale-Up: A Review. *Processes, 12*(8), 1635. https://www.mdpi.com/2227-9717/12/8/1635

Albuquerque, M. M., Martinez-Burgos, W. J., De Bona Sartor, G., Letti, L. A. J., De Carvalho, J. C., Soccol, C. R., & Medeiros, A. B. P. (2024). Advances and Perspectives in Biohydrogen Production from Palm Oil Mill Effluent. *Fermentation, 10*(3), 141.

Anjum, S., Aslam, S., Hussain, N., Bilal, M., Boczkaj, G., Smułek, W., Jesionowski, T., & Iqbal, H. M. N. (2023). Bioreactors and biophoton-driven biohydrogen production strategies. *International Journal of Hydrogen Energy, 48*(55), 21176-21188. https://doi.org/https://doi.org/10.1016/j.ijhydene.2023.01.363

Araujo, M. N., Vargas, S. R., Soares, L. A., Trindade, L. F., Fuess, L. T., & Adorno, M. A. T. (2024). Rapid method for determination of biogas composition by gas chromatography coupled to a thermal conductivity detector (GC-TCD). *International Journal of Environmental Analytical Chemistry, 104*(20), 8690-8707. https://doi.org/10.1080/03067319.2023.2210055

Arisht, S., Senan Mahmod, S., Abdul, P., Indera Luthfi, A. A., Takriff, M., Lay, C.-H., Silvamany, H., Sittijunda, S., & Jamaliah, M. (2022). Enhancing biohydrogen gas production in anaerobic system via comparative chemical pre-treatment on palm oil mill effluent (POME). *Journal of Environmental Management, 321,* 115892. https://doi.org/10.1016/j.jenvman.2022.115892

Arisht, S. N., Mahmod, S. S., Abdul, P. M., Indera Lutfi, A. A., Takriff, M. S., Lay, C. H., Silvamany, H., Sittijunda, S., & Jahim, J. M. (2022). Enhancing biohydrogen gas production in anaerobic system via comparative chemical pre-treatment on palm oil mill effluent (POME). *J Environ Manage, 321*, 115892. https://doi.org/10.1016/j.jenvman.2022.115892

Asvad, M., Hajinezhad, A., Jafari, A., & Moosavian, S. F. (2023). Multiscale kinetic modeling for biohydrogen production: A study on membrane bioreactors. International *Journal of Hydrogen Energy, 48*(76), 29641-29650. https://doi.org/https://doi.org/10.1016/j.ijhydene.2023.04.151

Batstone, D. J., Keller, J., Angelidaki, I., Kalyuzhnyi, S. V., Pavlostathis, S. G., Rozzi, A., Sanders, W., Siegrist, H., & Vavilin, V. A. (2002). The IWA anaerobic digestion model no 1 (ADM1). *Water Science and Technology, 45*(10), 65-73.

Bayu, A. I., Lestary, R. A., Dewayanto, N., Mellyanawaty, M., Wicaksono, A., Alvania Kartika, R. W., Sakka, D. F., Azis, M. M., & Budhijanto, W. (2022). Kinetic study of thermophilic anaerobic digestion of sugarcane vinasse in a single-stage continuous stirred tank reactor. *Results in Engineering, 14,* 100432. https://doi.org/https://doi.org/10.1016/j.rineng.2022.100432

Bechara, R. (2022). Improvements to the ADM1 based Process Simulation Model: Reaction segregation, parameter estimation and process optimization. *Heliyon, 8*(12), e11793. https://doi.org/https://doi.org/10.1016/j.heliyon.2022.e11793

Bouchareb, E. M., Derbal, K., Bedri, R., Slimani, K., Menas, S., Lazreg, H., Maaref, F., Ouabdelkader, S., Saheb, A., Bouaita, R., Bouchareb, R., & Dizge, N. (2024). Improving Biohydrogen Production by Dark Fermentation of Milk Processing Wastewater by Physicochemical and Enzymatic Pretreatments. *Applied Biochemistry and Biotechnology, 196*(5), 2741-2756. https://doi.org/10.1007/s12010-023-04619-2

Chen, S.-J., Chen, X., Hu, B.-B., Wei, M.-Y., & Zhu, M.-J. (2023). Efficient hydrogen production from sugarcane bagasse and food waste by thermophilic clostridiales consortium and Fe–Mn impregnated biochars. *Renewable Energy, 211,* 166-178. https://doi.org/https://doi.org/10.1016/j.renene.2023.04.114

Chen, Z., & Wang, L. (2024). Process simulation and evaluation of scaled-up biocatalytic systems: Advances, challenges, and future prospects. *Biotechnology Advances, 77,* 108470. https://doi.org/https://doi.org/10.1016/j.biotechadv.2024.108470

Couto, P. T., Eng, F., Bovio-Winkler, P., Cavalcante, W. A., Etchebehere, C., Fuentes, L., Nopens, I., Zaiat, M., & Ribeiro, R. (2022). Modeling of hydrogen and organic acid production using different concentrations of sugarcane vinasse under thermophilic conditions and a link with microbial community 16S rRNA gene sequencing data. *Journal of Cleaner Production, 370,* 133437. https://doi.org/https://doi.org/10.1016/j.jclepro.2022.133437

Couto, P. T., Eng, F., Naessens, W., Nopens, I., Zaiat, M., & Ribeiro, R. (2020). Modelling sugarcane vinasse processing in an acidogenic reactor to produce hydrogen with an ADM1-based model. *International Journal of Hydrogen Energy, 45*(11), 6217-6230. https://doi.org/https://doi.org/10.1016/j.ijhydene.2019.12.206

Dareioti, M. A., Vavouraki, A. I., & Kornaros, M. (2014). Effect of pH on the anaerobic acidogenesis of agroindustrial wastewaters for maximization of bio-hydrogen production: A lab-scale evaluation using batch tests. *Bioresource Technology, 162,* 218-227. https://doi.org/https://doi.org/10.1016/j.biortech.2014.03.149

Deb, N., Alam, M. Z., Rahman, T., Al-Khatib, M. a. F. R., Jami, M. S., & Mansor, M. F. B. (2023). Acid–Base Pretreatment and Enzymatic Hydrolysis of Palm Oil Mill Effluent in a Single Reactor System for Production of Fermentable Sugars. *International Journal of Polymer Science,* 2023(1), 8711491. https://doi.org/https://doi.org/10.1155/2023/8711491

Economou, C. N., Manthos, G., Zagklis, D., & Kornaros, M. (2024). ADM1-Based Modeling of Biohydrogen Production through Anaerobic Co-Digestion of Agro-Industrial Wastes in a Continuous-Flow Stirred-Tank Reactor System. *Fermentation, 10*(3), 138. https://www.mdpi.com/2311-5637/10/3/138

Emebu, S., Pecha, J., & Janáčová, D. (2022). Review on anaerobic digestion models: Model classification & elaboration of process phenomena. *Renewable and Sustainable Energy Reviews, 160,* 112288. https://doi.org/https://doi.org/10.1016/j.rser.2022.112288

Engliman, N. S., Aziz, A. H. A., Mansor, M. F., Abdul, P. M., Jahim, J. M., & Jamali, N. S. (2022). Kinetic study on the effect of substrate and micronutrient inhibition during anaerobic fermentation of biohydrogen. *Int J Curr Sci Res Rev, 5,* 13-25.

Greses, S., Tomás-Pejó, E., & González-Fernández, C. (2022). Food waste valorization into bioenergy and bioproducts through a cascade combination of bioprocesses using anaerobic open mixed cultures. *Journal of Cleaner Production, 372,* 133680. https://doi.org/https://doi.org/10.1016/j.jclepro.2022.133680

Izzi, A. Z., Wan Ishak, W. M. F., Yusuf, N. N. A. N., Alenezi, R. A., & Alias, N. A. (2023). Thermophilic biohydrogen production from optimized enzymatic pretreatment of palm oil mill effluent via box-behnken design. *Journal of Engineering Research, 11*(2), 100054. https://doi.org/https://doi.org/10.1016/j.jer.2023.100054

Keller, J., Rozzi, A., & Sanders, W. (2002). The IWA anaerobic digestion model no 1 (ADM1). *Water Science and Technology, 45*(10), 65-73.

Lee, H.-S., Xin, W., Katakojwala, R., Venkata Mohan, S., & Tabish, N. M. D. (2022). Microbial electrolysis cells for the production of biohydrogen in dark fermentation – A review. *Bioresource Technology, 363*, 127934. https://doi.org/https://doi.org/10.1016/j.biortech.2022.127934

Li, W., Lu, L., Cheng, C., Ren, N., Yang, S.-T., & Liu, M. (2022). Biohydrogen production from brown algae fermentation: Relationship between substrate reduction degree and hydrogen production. *Bioresource Technology, 364,* 128069. https://doi.org/https://doi.org/10.1016/j.biortech.2022.128069

Litti, Y. V., Potekhina, M. A., Zhuravleva, E. A., Vishnyakova, A. V., Gruzdev, D. S., Kovalev, A. A., Kovalev, D. A., Katraeva, I. V., & Parshina, S. N. (2022). Dark fermentative hydrogen production from simple sugars and various wastewaters by a newly isolated *Thermoanaerobacterium thermosaccharolyticum* SP-H2. *International Journal of Hydrogen Energy, 47*(58), 24310-24327. https://doi.org/https://doi.org/10.1016/j.ijhydene.2022.05.235

Mahmod, S. S., Jahim, J. M., & Abdul, P. M. (2017). Pretreatment conditions of palm oil mill effluent (POME) for thermophilic biohydrogen production by mixed culture. *International Journal of Hydrogen Energy, 42*(45), 27512-27522.

Martínez-Mendoza, L. J., Lebrero, R., Muñoz, R., & García-Depraect, O. (2022). Influence of key operational parameters on biohydrogen production from fruit and vegetable waste via lactate-driven dark fermentation. *Bioresource Technology, 364,* 128070. https://doi.org/https://doi.org/10.1016/j.biortech.2022.128070

Martínez, V. L., Salierno, G. L., García, R. E., Lavorante, M. J., Galvagno, M. A., & Cassanello, M. C. (2022). Biological Hydrogen Production by Dark Fermentation in a Stirred Tank Reactor and Its Correlation with the pH Time Evolution. *Catalysts, 12*(11), 1366. https://www.mdpi.com/2073-4344/12/11/1366

Mo, R., Guo, W., Batstone, D., Makinia, J., & Li, Y. (2023). Modifications to the anaerobic digestion model no. 1 (ADM1) for enhanced understanding and application of the anaerobic treatment processes – A comprehensive review. *Water Research, 244*, 120504. https://doi.org/https://doi.org/10.1016/j.watres.2023.120504

Montgomery, D. C. (2017). Design and analysis of experiments. John wiley & sons.

Mudzanani, K. E., Phadi, T. T., Iyuke, S. E., & Daramola, M. O. (2023). Enhancing Methane Production through Anaerobic Co-Digestion of Sewage Sludge: A Modified ADM1 Model Approach. *Fermentation, 9*(9), 833. https://www.mdpi.com/2311-5637/9/9/833

Ndayisenga, F., Yu, Z., Wang, B., Wu, G., Zhang, H., Phulpoto, I. A., Zhao, J., & Yang, J. (2022). Thermophilic-operating environment promotes hydrogen-producing microbial growth in a lignocellulose-fed DF-MEC system for enhanced biohydrogen evolution. *Process Safety and Environmental Protection, 167*, 213-224. https://doi.org/https://doi.org/10.1016/j.psep.2022.09.026

Núñez-Valenzuela, P., Ontiveros-Valencia, A., René Rangel-Méndez, J., Nieto-Delgado, C., & Razo-Flores, E. (2024). Extractive fermentation as a strategy to increase the co-production of H2 and carboxylates in dark fermentation. *Fuel, 362*, 130804. https://doi.org/https://doi.org/10.1016/j.fuel.2023.130804

Porninta, K., Khemacheewakul, J., Techapun, C., Phimolsiripol, Y., Jantanasakulwong, K., Sommanee, S., Mahakuntha, C., Feng, J., Htike, S. L., Moukamnerd, C., Zhuang, X., Wang, W., Qi, W., Li, F.-L., Liu, T., Kumar, A., Nunta, R., & Leksawasdi, N. (2024). Pretreatment and enzymatic hydrolysis optimization of lignocellulosic biomass for ethanol, xylitol, and phenylacetylcarbinol co-production using *Candida magnoliae*. *Frontiers in Bioengineering and Biotechnology, Volume 11*(2023). https://doi.org/10.3389/fbioe.2023.1332185

Priambodo, T. B., Hastuti, Z. D., Anindita, H. N., & Senda, S. P. (2024). The Impact of Thermal Pretreatment on Biohydrogen Production from Palm Oil Mill Effluent (POME) Through Hydrolysis-Acidogenesis. *Evergreen Joint Journal of Novel Carbon Resource Sciences & Green Asia Strategy, 11*(03): 1820-1833. https://www.tj.kyushu-u.ac.jp/evergreen/contents/EG2024-11_3_content/pdf/p1820-1833.pdf.

Punia, P., & Singh, L. (2024). Optimization of alkali pre-treatment of sweet sorghum [*Sorghum bicolor* (L.) Moench] residue to improve enzymatic hydrolysis for fermentable sugars. *Waste Management Bulletin, 2*(1), 131-141. https://doi.org/https://doi.org/10.1016/j.wmb.2023.12.007

Qi, C., Cao, D., Gao, X., Jia, S., Yin, R., Nghiem, L. D., Li, G., & Luo, W. (2023). Optimising organic composition of feedstock to improve microbial dynamics and symbiosis to advance solid-state anaerobic co-digestion of sewage sludge and organic waste. *Applied Energy, 351*, 121857. https://doi.org/https://doi.org/10.1016/j.apenergy.2023.121857

Rice, E. W., Baird, R. B., Eaton, A. D., & Clesceri, L. S. (2012). Standard methods for the examination of water and wastewater.

Sanghvi, A. H., Manjoo, A., Rajput, P., Mahajan, N., Rajamohan, N., & Abrar, I. (2024). Advancements in biohydrogen production – a comprehensive review of technologies, lifecycle analysis, and future scope. *RSC Advances, 14*(49), 36868-36885. https://doi.org/10.1039/D4RA06214K

Segura, T., Zanoni, P., Brémond, U., Lucet--Bérille, C., Pradel, A., Escudié, R., & Steyer, J.-P. (2025). Modelling anaerobic digestion of agricultural waste: From lab to full scale. *Waste Management, 200*, 114739. https://doi.org/https://doi.org/10.1016/j.wasman.2025.114739

Shi, L., Aoues, Y., & Leveneur, S. (2024). Impact of aleatory and epistemic uncertainties on thermal risk and production assessment: Application to the hydrogenation of levulinic acid and butyl levulinate. *Journal of Loss Prevention in the Process Industries, 89,* 105317. https://doi.org/https://doi.org/10.1016/j.jlp.2024.105317

Sim, X. Y., Tan, J. P., He, N., Yeap, S. K., Hui, Y. W., Luthfi, A. A. I., Manaf, S. F. A., Bukhari, N. A., & Jamali, N. S. (2023). Unraveling the effect of redox potential on dark fermentative hydrogen production. *Renewable and Sustainable Energy Reviews,* 187, 113755. https://doi.org/https://doi.org/10.1016/j.rser.2023.113755

Singh, H., Tomar, S., Qureshi, K. A., Jaremko, M., & Rai, P. K. (2022). Recent Advances in Biomass Pretreatment Technologies for Biohydrogen Production. *Energies, 15*(3), 999. https://www.mdpi.com/1996-1073/15/3/999

Singh, R., Hans, M., Kumar, S., & Yadav, Y. K. (2023). Thermophilic Anaerobic Digestion: An Advancement towards Enhanced Biogas Production from Lignocellulosic *Biomass. Sustainability, 15*(3), 1859. https://www.mdpi.com/2071-1050/15/3/1859

Song, G., Bai, Y., Pan, Z., Liu, D., Qin, Y., Zhang, Y., Fan, Z., Li, Y., & Madadi, M. (2024). Enhancing fermentable sugar production from sugarcane bagasse through surfactant-assisted ethylene glycol pretreatment and enzymatic hydrolysis: Reduced temperature and enzyme loading. *Renewable Energy, 227,* 120515. https://doi.org/https://doi.org/10.1016/j.renene.2024.120515

Vera, G., Feijoo, F. A., & Prieto, A. L. (2023). A Mechanistic Model for Hydrogen Production in an AnMBR Treating High Strength Wastewater. *Membranes, 13*(11), 852. https://www.mdpi.com/2077-0375/13/11/852

Wang, J., & Guo, X. (2024). The Gompertz model and its applications in microbial growth and bioproduction kinetics: Past, present and future. *Biotechnology Advances, 72*, 108335. https://doi.org/https://doi.org/10.1016/j.biotechadv.2024.108335

Yang, E., Chon, K., Kim, K.-Y., Le, G. T. H., Nguyen, H. Y., Le, T. T. Q., Nguyen, H. T. T., Jae, M.-R., Ahmad, I., Oh, S.-E., & Chae, K.-J. (2023). Pretreatments of lignocellulosic and algal biomasses for sustainable biohydrogen production: Recent progress, carbon neutrality, and circular economy. *Bioresource Technology, 369,* 128380. https://doi.org/https://doi.org/10.1016/j.biortech.2022.128380

Zagrodnik, R., Duber, A., & Seifert, K. (2022). Dark-fermentative hydrogen production from synthetic lignocellulose hydrolysate by a mixed bacterial culture: The relationship between hydraulic retention time and pH conditions. *Bioresource Technology, 358*, 127309. https://doi.org/https://doi.org/10.1016/j.biortech.2022.127309

Zainal, B. S., Yu, K. L., Ong, H. C., Mohamed, H., Ker, P. J., Abdulkreem-Alsultan, G., Taufiq-Yap, Y. H., & Mahlia, T. M. I. (2024). Synergising hydrothermal pre-treatment and biological processes for enhancing biohydrogen production from palm oil mill effluent. *Process Safety and Environmental Protection, 192,* 424-436. https://doi.org/https://doi.org/10.1016/j.psep.2024.10.024

Zainal, B. S., Zaini, S., Zinatizadeh, A. A., Mohd, N. S., Ibrahim, S., Ker, P. J., & Mohamed, H. (2023). Preliminary Investigation of Different Types of Inoculums and Substrate Preparation for Biohydrogen Production. *Fermentation, 9*(2), 127. https://www.mdpi.com/2311-5637/9/2/127

Zhang, H., Yuan, W., Dong, Q., Wu, D., Yang, P., Peng, Y., Li, L., & Peng, X. (2022). Integrated multi-omics analyses reveal the key microbial phylotypes affecting anaerobic digestion performance under ammonia stress. *Water Research, 213,* 118152. https://doi.org/https://doi.org/10.1016/j.watres.2022.118152

Zhu, J., Song, W., Chen, X., & Sun, S. (2023). Integrated process to produce biohydrogen from wheat straw by enzymatic saccharification and dark fermentation. *International Journal of Hydrogen Energy, 48*(30), 11153-11161. https://doi.org/https://doi.org/10.1016/j.ijhydene.2022.05.056

